

# Discovery of 47-s pulsations in the X-ray source 1RXS J225352.8+624354

P. Esposito,<sup>1\*</sup> G. L. Israel,<sup>2</sup> L. Sidoli,<sup>1</sup> E. Mason,<sup>3</sup> G. A. Rodríguez Castillo,<sup>2,4</sup>  
J. P. Halpern,<sup>5</sup> A. Moretti<sup>6</sup> and D. Götz<sup>7</sup>

<sup>1</sup>*Istituto di Astrofisica Spaziale e Fisica Cosmica - Milano, INAF, via E. Bassini 15, I-20133 Milano, Italy*

<sup>2</sup>*Osservatorio Astronomico di Roma, INAF, via Frascati 33, I-00040 Monteporzio Catone, Italy*

<sup>3</sup>*Space Telescope Science Institute, 3700 San Martin Drive, Baltimore, MD 21218, USA*

<sup>4</sup>*Dipartimento di Fisica, Università di Roma “La Sapienza”, p.le A. Moro 2, I-00185 Roma, Italy*

<sup>5</sup>*Astronomy Department, Columbia University, 550 West 120th Street, New York, NY 10027-6601, USA*

<sup>6</sup>*Osservatorio Astronomico di Brera, INAF, via Brera 28, I-20121 Milano, Italy*

<sup>7</sup>*AIM CEA/Irfu/Service d’Astrophysique, Orme des Merisiers, F-91191 Gif-sur-Yvette, France*

Accepted 2013 May 15. Received 2013 May 14; in original form 2013 April 17

## ABSTRACT

We report on the discovery of pulsations at a period of  $\sim 47$  s in the persistent X-ray source 1RXS J225352.8+624354 (1RXS J2253) using five *Chandra* observations performed in 2009. The signal was also detected in *Swift* and *ROSAT* data, allowing us to infer over a 16-yr baseline an average, long-term period increasing rate of  $\approx 17$  ms per year and therefore to confirm the signal as the spin period of an accreting, spinning-down neutron star. The pulse profile of 1RXS J2253 ( $\sim 50$ – $60\%$  pulsed fraction) is complex and energy independent (within the statistical uncertainties). The 1–10 keV *Chandra* spectra are well fit by an absorbed power-law model with  $\Gamma \sim 1.4$  and observed flux of  $(2\text{--}5) \times 10^{-12}$  erg cm $^{-2}$  s $^{-1}$ . The source was also detected by *INTEGRAL* in the 17–60 keV band at a persistent flux of  $\sim 6 \times 10^{-12}$  erg cm $^{-2}$  s $^{-1}$ , implying a spectral cut off around 15 keV. We also carried out optical spectroscopic follow-up observations of the 2MASS counterpart at the Nordic Optical Telescope. This made it possible to first classify the companion of 1RXS J2253 as a B0–III–Ve (most likely a B1Ve) star at a distance of about 4–5 kpc (favouring an association with the Perseus arm of the Galaxy). The latter finding implies an X-ray luminosity of  $\sim 3 \times 10^{34}$  erg s $^{-1}$ , suggesting that 1RXS J2253 is a new member of the sub-class of low-luminosity long-orbital-period persistent Be/X-ray pulsars in a wide and circular orbit (such as X Persei).

**Key words:** stars: emission-line, Be – stars: individual: 2MASS J22535512+6243368 – X-rays: binaries – X-rays: individual: 1RXS J225352.8+624354 (CXOU J225355.1+624336, 1WGA J2253.9+6243, IGR J22534+6243)

## 1 INTRODUCTION

Every time a new X-ray mission is launched, many serendipitous X-ray sources of unknown nature are usually discovered. Among them, some may suddenly become objects of interest because they display outbursts/flares or are recognised to be the X-ray counterpart of sources discovered at other wavelengths, but most of them, especially the faintest ones, can remain unidentified for years. Sometimes they are ‘re-discovered’ by the next X-ray missions or by systematic archival searches for specific signatures (such as flux variability, multiwavelength associations or pulsations).

The identification of detected sources with still unknown nature is a fundamental step towards the study of the different populations of Galactic and extragalactic X-ray sources, and

can lead to surprising results. Examples are the discovery of RX J0806.3+1527, the double-degenerate ultracompact binary with the shortest known orbital period (5.4 minutes; Israel et al. 1999, 2002; Ramsay, Hakala & Cropper 2002), or the realisation of the existence of a potentially large population of ‘dormant’ magnetars (e.g. Rea & Esposito 2011 and references therein). This was also the case of the supergiant fast X-ray transients (SFXTs), a class of hard X-ray transients discovered by the *INTEGRAL* satellite (Sguera et al. 2005); in several cases in fact, SFXTs were found to be associated with objects listed in catalogues of faint soft-X-ray sources from past missions (mostly *ASCA* and *BeppoSAX*).

The discovery of coherent X-ray pulsations, in particular, is a key element to understand the nature of a source. The *Chandra ACIS Timing Survey at Brera And Rome astronomical observatories* (CATS@BAR) is a project aimed at the exploitation of Advanced CCD Imaging Spectrometer (ACIS; Garmire et al.

\* E-mail: paoloesp@iasf-milano.inaf.it

2003) archival data from the *Chandra* mission (Weisskopf et al. 2002).<sup>1</sup> As of 2013 February 28, approximately 8,750 Timed-Exposure observations were retrieved (data taken with gratings and in Continuous-Clocking mode were not included in the analysis) and about 400,000 light curves were extracted. For the 85,000 light curves with more than  $\sim 150$  photons, Fourier power spectra were computed and analysed. These were searched for coherent or quasi-coherent signals in a systematic and automatised way by applying the detection algorithm described in Israel & Stella (1996). Among the about 30 new candidate X-ray pulsators showing signals with high confidence level ( $>4.5\sigma$ ) found so far (Israel et al., in preparation), there is 1RXS J225352.8+624354 (hereafter 1RXS J2253), which has a period of  $\sim 47$  s.

The source was discovered by *ROSAT* and included in the All-Sky Survey Faint Source Catalogue (Voges et al. 2000; 1RXS J225352.8+624354) and in the WGA Catalog (White, Giommi & Angelini 1994; 1WGA J2253.9+6243). 1RXS J2253 was later suggested to be a low-luminosity hard X-ray binary by Suchkov & Hanisch (2004). More recently, Landi et al. (2012) pointed out that 1RXS J2253 is the X-ray counterpart of the *INTEGRAL* source IGR J22534+6243 (Krivonos et al. 2012). The 47-s pulsation of 1RXS J2253 was then discovered and reported by Halpern 2012 and independently (within the CATS@BAR project) by Israel & Rodríguez (2012). It was also noticed that the position of 1RXS J2253 is consistent with that of the infrared source 2MASS J22535512+6243368 (Halpern 2012; Landi et al. 2012), suggesting a high-mass stellar companion. The high-mass X-ray binary (HMXB) classification was strengthened by Masetti et al. (2012) who performed a follow-up optical observation in 2012 June and obtained a 4000–8000 Å spectrum characterised by a highly-reddened, intrinsically-blue continuum with H $\alpha$ , H $\beta$  and H $\epsilon$  emission lines. Here we report on the spectral and timing analysis of the archival *ROSAT*, *Swift*, and *Chandra* observations that serendipitously imaged the field of 1RXS J2253 across  $\sim 16$  years. As a further step toward the classification of 1RXS J2253, we also observed it with the 2.5-m Nordic Optical Telescope in the Canary Islands on two nights in 2012 December.

## 2 OBSERVATIONS AND DATA REDUCTION

### 2.1 *Chandra*

*Chandra* imaged the position of 1RXS J2253 five times in 2009 (see Table 1) in a campaign devoted to a portion of the Cepheus OB3 molecular cloud (see Allen et al. 2012). The data were acquired with the ACIS instrument in Very Faint imaging (Timed Exposure) mode (time resolution:  $\sim 3.2$  s).

The data were reprocessed with the Chandra Interactive Analysis of Observations software (CIAO, version 4.4) using the calibration files available in the *Chandra* CALDB 4.4.8 database. The scientific products were extracted following standard procedures, adopting extraction regions of  $\sim 6$ –25 arcsec radii (depending on the off-axis angle, around 15 arcmin in most pointings) for the source counts. In particular the spectra, the spectral redistribution matrices and the ancillary response files were created using SPEXTRACT. For the timing analysis, we applied the Solar system barycentre correction to the photon arrival times with AXBARY.

### 2.2 *Swift*

*Swift* serendipitously observed 1RXS J2253 in two contiguous observations carried out to follow the afterglow of the gamma-ray burst GRB 060421 (Goat et al. 2006). The net exposure of the X-ray Telescope (XRT; Burrows et al. 2005) data was 73.0 ks in photon counting (PC; full imaging, time resolution:  $\sim 2.5$  s) mode and 1.8 ks in windowed timing (WT; one-dimensional strip readout, time resolution:  $\sim 1.8$  ms) mode; since the observation was pointed at GRB 060421, only the PC data can be used to study 1RXS J2253 (see Table 1). The Ultraviolet/Optical Telescope (UVOT; Roming et al. 2005) observed the field simultaneously with its optical and ultraviolet (UV) filters (see Table 5).

The *Swift* data were processed and screened with standard procedures and quality cuts using FTOOLS in the HEASOFT (version 6.12) software package and the calibration files in the 2012-04-02 CALDB release. The XRT photon arrival times were corrected to the Solar system barycenter with BARYCORR. The XRT source counts were extracted within a 20-pixel radius (one XRT pixel corresponds to about 2.36 arcsec). For the X-ray spectral fitting, the ancillary response files were generated with XRTMKARF accounting for different extraction regions, vignetting, point-spread function corrections, and dead, hot or warm pixels (Moretti et al. 2005). The UVOT photometry<sup>2</sup> was performed with the UVOTSOURCE task, which calculates the magnitudes through aperture photometry.

### 2.3 *ROSAT*

The position of 1RXS J2253 occurred within the *ROSAT* Position Sensitive Proportional Counter (PSPC; Pfeffermann et al. 1987) field of view in four pointings carried out between July 1992 and June 1993. However, owing to large off-axis angles and/or short duration, in three out of the four observations the exposures provide too few photons for meaningful analyses. The only observation useful for timing and spectral analysis was carried out in June 1993 (obs. ID RP500321N00, see Table 1) for an effective exposure time of  $\sim 18$  ks.

The event lists and spectra for 1RXS J2253 and the background were extracted from circles of  $\sim 1$  arcmin radius. The solar system barycenter correction to the photon arrival times was applied with the FTOOLS tasks BCT and ABC. For the spectroscopy, we used the spectral redistribution matrix PSPCB\_GAIN2\_256.RMF, while the ancillary response file was generated with PCARF.

### 2.4 Nordic Optical Telescope

1RXS J2253 was observed at the 2.5-m Nordic Optical Telescope (NOT) equipped with the Andaluia Faint Object Spectrograph and Camera, (ALFOSC) on 2012 December 26 and 30. We used the grism N.7 and slit of 0.5 arcsec, covering the wavelength range  $\sim 3800$ –6800 Å at a resolution of 4.4 Å or  $\sim 237$  km s<sup>-1</sup>.<sup>3</sup> We obtained four spectra per night, each of 900 s exposure time. The observations had attached arc-lamp exposure and flat field.

The data were reduced using IRAF (Tody 1993) packages and

<sup>1</sup> See <http://www.mporzio.astro.it/gianluca/resultss.html> for the analogous *Swift* project, *Swift Automatic Timing ANALysis of Serendipitous Sources at Brera And Roma astronomical observatories* (SATANASS@BAR).

<sup>2</sup> See Poole et al. (2008) for an overview of the UVOT photometric system and Breeveld et al. (2011) for the most updated zero-points and count rate to flux conversion factors.

<sup>3</sup> As measured on the sky emission lines.

**Table 1.** Observations used for this work.

Instrument	Obs.ID	Start date (YYYY-MM-DD)	Duration (ks)	Net count rate <sup>a</sup> (counts s <sup>-1</sup> )
<i>ROSAT</i> /PSPC-B	RP900425N00	1992-07-29	4.3	$(1.1 \pm 0.2) \times 10^{-2}$
<i>ROSAT</i> /PSPC-B	RP900425A01	1992-12-27	6.4	$(1.7 \pm 0.3) \times 10^{-2}$
<i>ROSAT</i> /PSPC-B	RP500321N00	1993-06-18	18.5	$(1.17 \pm 0.08) \times 10^{-2}$
<i>ROSAT</i> /PSPC-B	RP500322N00	1993-06-20	15.7	$(0.8 \pm 0.3) \times 10^{-2}$
<i>Swift</i> /XRT	00206257000	2006-04-21	25.0	$(4.2 \pm 0.1) \times 10^{-2}$
<i>Swift</i> /XRT	00206257001	2006-04-21	48.0	$(3.06 \pm 0.08) \times 10^{-2}$
<i>Chandra</i> /ACIS-S	9920	2009-04-16	27.7	$(6.6 \pm 0.2) \times 10^{-2}$
<i>Chandra</i> /ACIS-I	10811	2009-04-28	24.4	$(6.5 \pm 0.2) \times 10^{-2}$
<i>Chandra</i> /ACIS-I	10812	2009-05-03	24.8	$(6.0 \pm 0.2) \times 10^{-2}$
<i>Chandra</i> /ACIS-S	10810	2009-05-07	22.8	$(9.1 \pm 0.2) \times 10^{-2}$
<i>Chandra</i> /ACIS-I	9919	2009-05-08	22.5	$(5.8 \pm 0.2) \times 10^{-2}$

<sup>a</sup> Observed count rates (not corrected for PSF and effective area effects) in the energy ranges: 1–2.4 keV for *ROSAT* and 1–10 keV for *Swift* and *Chandra*.

tasks and following standard procedures. However, we did not apply the flat field correction due to the fact that the flats were insufficient in number and, in one case, count level. Hence, we did not correct for the pixel-to-pixel variation, nor we removed the fringing at  $\lambda \geq 6300 \text{ \AA}$ . However, we removed the spectrograph signatures (low frequency variations) during the flux calibration step: the spectro-photometric standard stars were observed with exactly the same set up. In particular we observed both BD +17° 4708 and Feige 110, during each night. Fluxes are not absolute as both the target object and the spectrophotometric standard star were affected by slit losses which we could not estimate and correct for.

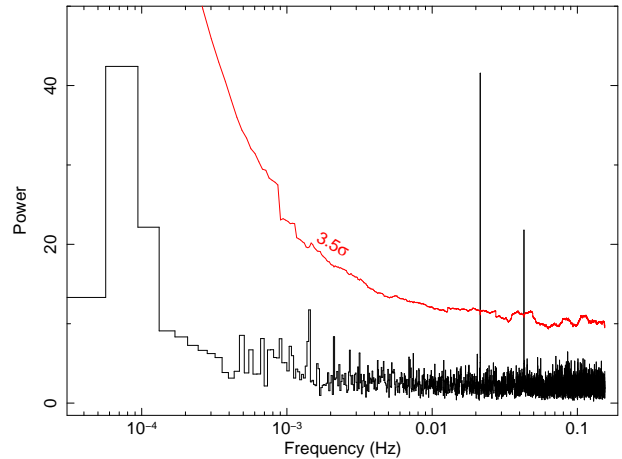
### 3 TIMING ANALYSIS AND RESULTS

The inspection of the X-ray light curves showed evidence of moderate variability on a time-scale of a few ks. The root-mean-square (rms) fractional variation (defined as the rms variation normalised by the average count rate) was  $52 \pm 5\%$  in observation *Swift*/7000, and  $47 \pm 6\%$  in *Swift*/7001 (measured in 1–10 keV light curves, bin size of 500 s). In the *Chandra* observations (1–10 keV, 500 s bin size) it was, in chronological order,  $22 \pm 4\%$  (obs. 9920),  $34 \pm 4\%$  (10811),  $29 \pm 4\%$  (10812),  $33 \pm 4\%$  (10810), and  $23 \pm 4\%$  (9919). For the *ROSAT* observation 500321 we could only place an upper limit of  $\sim 40\%$  ( $3\sigma$  c.l.) for bin sizes from 0.5 to 5 ks (1–2.4 keV).

As anticipated,  $\sim 46.7$ -s coherent pulsations from 1RXS J2253 were found within the CATS@BAR project using the whole *Chandra* dataset. Fig. 1 shows the discovery periodogram where two peaks, corresponding to the fundamental ( $\nu_1 = 1/P \simeq 0.0214$  Hz) and the second ( $\nu_2 = 1/(2P)$ ) harmonics, stand well above the significance threshold. For the analysis of the coherent period that follows, the photon arrival times were transformed to Barycentric Dynamical Time (TDB) using the 2MASS coordinates of the optical/infrared counterpart listed in Table 3.

The signal is easily detectable also in the 2006 *Swift* dataset (since the two observations were contiguous, we treated them as a single one), where we measured by the  $Z_2^2$  test (e.g. Buccheri et al. 1983), which optimises the pulsed power, a period of 46.6145(5) s. The pulsed fraction (defined as  $(M - m)/(M + m)$ , where  $M$  and  $m$  are the observed background-subtracted count rates at the peak and at the minimum, respectively) of the folded profile (Fig. 2) is  $45 \pm 5$  percent in the 1–10 keV range.

In the case of the *ROSAT*/PSPC data, considering the  $\sim 13$  years elapsed between *ROSAT* and *Swift* observations, we carried


**Figure 1.** Fourier power spectrum of the whole *Chandra* dataset of 1RXS J2253 (0.5–10 keV). The red stepped line corresponds to  $3.5\sigma$  confidence level threshold for potential signals (computed taking into accounts the number of trial equal to the number of frequency bin of the spectrum). The two peaks above the threshold are the fundamental and the second harmonics of the 46.7-s signal.

**Table 2.** *Chandra* timing of 1RXS J2253.

Obs.ID	Start Epoch MJD	Period (s)	$Z_2^2$	Pulsed fraction (%)
9920	54937.446	46.6784(37)	94.7	$55 \pm 7$
10811	54949.292	46.6718(44)	94.7	$60 \pm 6$
10812	54954.072	46.6703(37)	90.4	$48 \pm 7$
10810	54958.855	46.6701(37)	96.2	$47 \pm 6$
9919	54959.143	46.6646(41)	79.8	$47 \pm 7$

out a period search in an interval set by a period derivative  $\pm \dot{P}$ , assuming a maximum spin-up/down intensity  $|\dot{P}| = 5 \times 10^{-8} \text{ s s}^{-1}$ . A significant peak (6.4 $\sigma$  c.l. in about  $10^3$  trial periods) was found in a  $Z_2^2$  periodogram at a best period of 46.406(5) s (see the folded profile in Fig. 2). The corresponding pulsed fraction is  $65 \pm 11$  percent (0.1–2.4 keV).

For each ACIS observation listed in Table 1 we extracted source photons in the 1–10 keV band using an aperture of radius  $10''$  or  $20''$  as appropriate. We used the  $Z_2^2$  test to measure the pe-

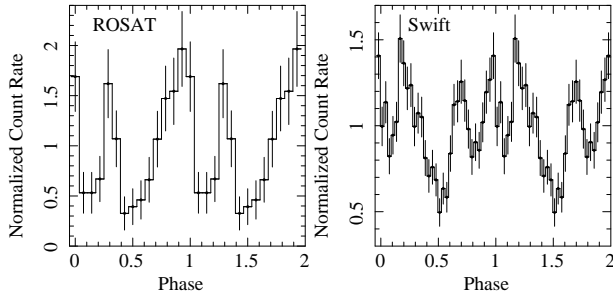


**Figure 2.** *ROSAT*/PSPC (0.1–2.4 keV) and *Swift*/XRT (1–10 keV) normalised pulse profiles of 1RXS J2253. Both profiles have been aligned so that the minimum phase coincides with that of the *Chandra* minimum in Fig. 3.

**Table 3.** *Chandra* ephemeris of 1RXS J2253.

Parameter	Value
R.A. (J2000.0) <sup>a</sup>	22 <sup>h</sup> 53 <sup>m</sup> 55 <sup>s</sup> .12
Decl. (J2000.0) <sup>a</sup>	+62° 43′ 36″.8
Epoch of ephemeris (MJD TDB) <sup>b</sup>	54954.00050
Valid range of dates (MJD)	54937–54959
Frequency, $f$ (Hz)	0.02142536(2)
Frequency derivative, $\dot{f}$ (Hz s <sup>-1</sup> )	$-6.1(4) \times 10^{-13}$
Period, $P$ (s)	46.67366(4)
Period derivative, $\dot{P}$ (s s <sup>-1</sup> )	$1.33(9) \times 10^{-9}$

<sup>a</sup> 2MASS coordinates of optical/infrared counterpart.

<sup>b</sup> Epoch of pulse minimum (phase 0.5) in Fig. 3.

riods in the individual observations (Table 2), and to bootstrap a coherent ephemeris that links all of them. Beginning with the last two observations, which were contiguous over May 7–8 (Obs.IDs 10810 and 9919), it was possible to work backwards in time and add Obs.ID 10812 on May 3 and Obs.ID 10811 on April 28 to the ephemeris, refining the period as each additional observation was included. It was not possible to extrapolate further back to Obs.ID 9920 on April 16 using a linear ephemeris (constant period), as the phase of that observation deviated by  $\approx 0.6$  cycles from the predicted phase. However, a fit including a period derivative accurately predicted its phase, and resulted in the quadratic ephemeris given in Table 3. Figure 3 shows the pulse profiles folded according to this ephemeris.

The fit period derivative,  $\dot{P} = 1.3 \times 10^{-9} \text{ s s}^{-1}$ , may have contributions from both secular spin-down and orbital acceleration, as we show here. The long-term spin-down rate is  $\approx 5.3 \times 10^{-10} \text{ s s}^{-1}$  (Fig. 4). This is only  $\approx 40\%$  of the  $\dot{P}$  required to fit the series of *Chandra* observations, which means that orbital acceleration contributes to the *Chandra* timing over 22 days. The kinematic effect may be estimated assuming  $M_x = 1.4 M_\odot$  for the neutron star in a circular orbit around a Be star companion (see Sect. 5.1) of mass  $M_c = 20 M_\odot$ . The contribution of acceleration to  $\dot{P}$  is

$$\dot{P}_k = 1.4 \times 10^{-8} \left( \frac{P_{\text{orb}}}{100 \text{ d}} \right)^{-4/3} \left( \frac{M_c}{20 M_\odot} \right)^{1/3} \left( \frac{P}{46.7 \text{ s}} \right) (1+q)^{-2/3} \sin i \sin \phi, \quad (1)$$

where  $q = M_x/M_c$  is the mass ratio,  $i$  is the inclination of the binary, and  $\phi$  is the orbital phase of the companion. Evidently, the orbital period  $P_{\text{orb}}$  is significantly longer than the 22 day span of

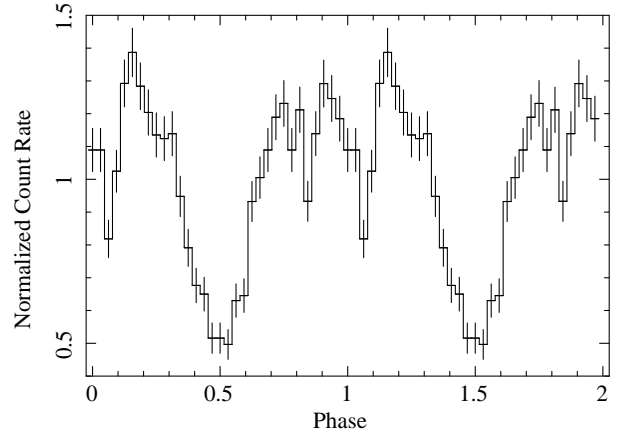


**Figure 3.** Normalised pulse profiles of 1RXS J2253 in the 1–10 keV band from *Chandra*, obtained by folding all data with the ephemeris in Table 3. The TDB epoch of pulse minimum (phase 0.5) is MJD 54954.00050.

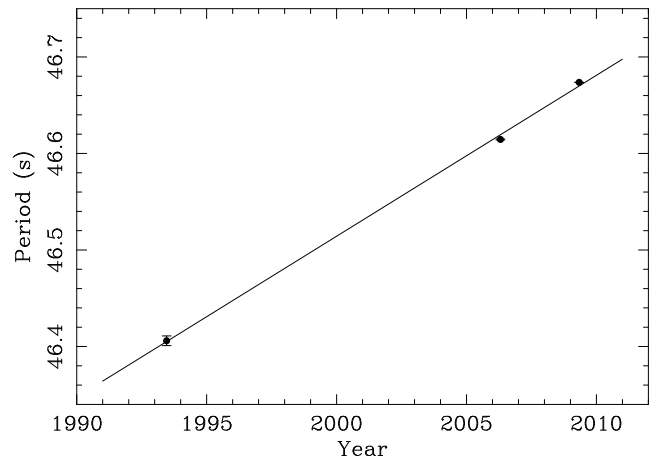


**Figure 4.** Long term spin-down of 1RXS J2253 from *ROSAT*, *Swift*, and *Chandra*. The systematic error on  $P$  due to orbital motion is  $\approx 0.02 \text{ s}$  (Eq. 2), which is larger than the measurement error on each point. Therefore, a simple least-squares fit is employed, yielding a mean  $\dot{P} = 5.3 \times 10^{-10} \text{ s s}^{-1}$ .

the *Chandra* observations because the observed  $\dot{P} = 1.3 \times 10^{-9} \text{ s s}^{-1}$  is small and constant to within  $\sim 10\%$  over this interval. Eq. 1 also implies that  $P_{\text{orb}} < 800$  days in order to provide the required acceleration. While orbital acceleration may account for the *Chandra* measured  $\dot{P}$ , the monotonic increase in spin period between *ROSAT*, *Swift*, and *Chandra* timings over 16 years cannot be due to orbital motion, since the total observed range in period is  $\Delta P \approx 0.27 \text{ s}$ , while the kinematic effect provides only

$$\Delta P_k = -0.019 \left( \frac{P_{\text{orb}}}{100 \text{ d}} \right)^{-1/3} \left( \frac{M_c}{20 M_\odot} \right)^{1/3} \left( \frac{P}{46.7 \text{ s}} \right) (1+q)^{-2/3} \sin i \cos \phi \text{ s}. \quad (2)$$

The *ROSAT* pulse shape, which is shown in Fig. 2, is dominated by two asymmetric peaks which are energy independent within the PSPC energy range (0.1–2.4 keV). In Fig. 3 we show the epoch-folded *Chandra* pulse profiles obtained using the ephemeris of Table 3. To assess the significance of the pulse shape variations through the high-count-statistics five *Chandra* data sets (Fig. 3),

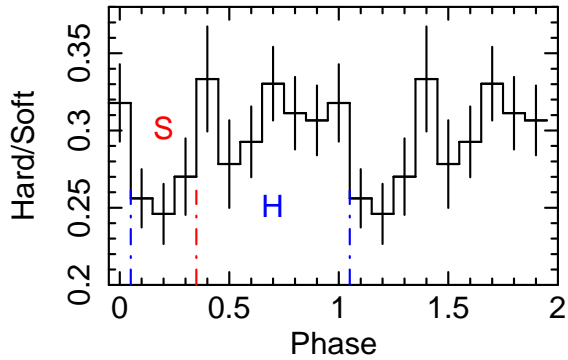


**Figure 5.** *Chandra* hardness ratio as function of the phase. The ratio was computed selecting soft photons in the 1–4.5 keV and hard photons in the 4.5–10 keV range. Phases are aligned with those of Fig. 3. The vertical lines and the labels indicate the phase intervals used for the phase-resolved spectroscopy (see text).

we compared each of the folded light curves with all the others by using a bidimensional Kolmogorov-Smirnov test (e.g. Press et al. 1992). The results show that all profiles are consistent with coming from the same distribution; the most significantly different pair of profiles are those of observations 10811 and 10810, which differs at a  $\sim 1.5\sigma$  confidence level. We compared in the same way the total *Chandra* and *Swift* (Fig. 2) profiles. Taking into account the unknown relative phase alignment, the probability that they come from the same underlying distribution is about 6.1 per cent. The pulse profiles do not show dramatic shape variations with energy, but a hardness-ratio analysis suggests some spectral variability along the spin phase (see Fig. 5). In fact the emission appears to be slightly harder during the minimum-rise part of the profile than at the decline phases.

#### 4 X-RAY SPECTRAL ANALYSIS AND RESULTS

Spectral fitting was carried out with XSPEC v.12.7 (Arnaud 1996). For each observation we extracted an average spectrum. A simple power-law model (modified for the interstellar absorption) provides an acceptable fit for all the data sets (see Table 4 for a summary of the spectral analysis). The average measured absorbing column corresponds to  $\sim 1.9 \times 10^{22} \text{ cm}^{-2}$  and the power law is rather hard, with an average photon index  $\Gamma \sim 1.4$ ; in the *Swift* and *Chandra* observations, the observed flux varies from  $\sim 2.4 \times 10^{-12}$  to  $\sim 4.5 \times 10^{-12} \text{ erg cm}^{-2} \text{ s}^{-1}$ .

Inspection of the energy-resolved light curves did not reveal neat spectral variations correlated with the source intensity. On the other hand, the hardness ratio analysis presented in Sect. 3 suggests some spectral variations with the spin phase. For each *Chandra* observation we extracted ‘soft’ and ‘hard’ spectra in two intervals chosen following the hardness ratio variations (see Fig. 5). A simultaneous fit of the spectra with an absorbed power-law model ( $\chi^2_\nu = 1.04$  for 327 dof) confirms a moderate hardening in the minimum-rise part of the profile, with an average power-law photon index  $\Gamma_H = 1.26 \pm 0.06$  to be compared with  $\Gamma_S = 1.4 \pm 0.1$  during the decline phases. We also produced a bidimensional histogram of the distribution of counts versus energy and phase to look for spectral features in the X-ray emission of 1RXS J2253, but none was found.

The hard-X-ray counterpart to 1RXS J2253 has been identified with *INTEGRAL* (IGR J22534+6243; Krivonos et al. 2012;

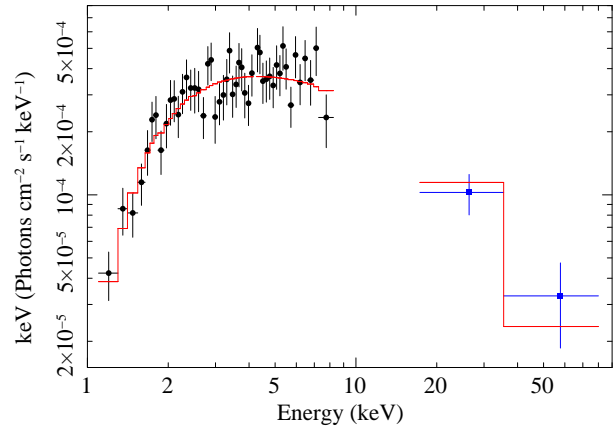


**Figure 6.** Broad-band soft and hard X unfolded model and (absorbed cut-off power law) spectrum ( $EF(E)$ ) of 1RXS J2253. For clarity, we show only the *Swift* (black dots) and *INTEGRAL* (blue squares) data.

Landi et al. 2012) in the IBIS 9-year Galactic Hard-X-Ray Survey (Perseus Arm). The reported source flux in the 17–60 keV energy band is  $(6 \pm 1) \times 10^{-12} \text{ erg cm}^{-2} \text{ s}^{-1}$ . The extrapolation in this hard-X-ray band of the power-law spectrum that describes the 1–10 keV data overestimates the *INTEGRAL* flux by a factor  $\sim 2$ . We built an IBIS/ISGRI (Ubertini et al. 2003; Lebrun et al. 2003) spectrum starting from the count rates in the 17–80 keV energy bands published by Krivonos et al. (2012) and rebinned the ISGRI response matrix in order to cope with the energy bands. A good simultaneous fit of the average 1–10 keV and *INTEGRAL* data ( $\chi^2_\nu = 1.01$  for 338 dof) can be obtained by using an absorbed cut-off power law (see Fig 6). The resulting spectral parameters are absorption  $N_H = (1.6 \pm 0.1) \times 10^{22} \text{ cm}^{-2}$ , photon index  $\Gamma = 1.0 \pm 0.1$ , cut-off energy  $E_C = 15 \pm 4 \text{ keV}$ , and 1–60 keV unabsorbed flux of  $\approx 1.2 \times 10^{-11} \text{ erg cm}^{-2} \text{ s}^{-1}$  (the 17–60 keV flux is  $\approx 5 \times 10^{-12} \text{ erg cm}^{-2} \text{ s}^{-1}$ ). This spectrum (slope and high energy cut-off) is typical of X-ray accreting pulsars (e.g. White et al. 1983).

#### 5 OPTICAL AND ULTRAVIOLET ANALYSIS AND RESULTS

As observed by Landi et al. (2012) and Halpern (2012), the X-ray position of 1RXS J2253 is consistent with that of the Two-Micron All-Sky Survey (2MASS; Skrutskie et al. 2006) source 2MASS 22535512+6243368 (see Table 5 for its magnitudes). The next closest source to 1RXS J2253, 2MASS 22535500+6243412, lies  $\sim 4.4$  arcsec away.

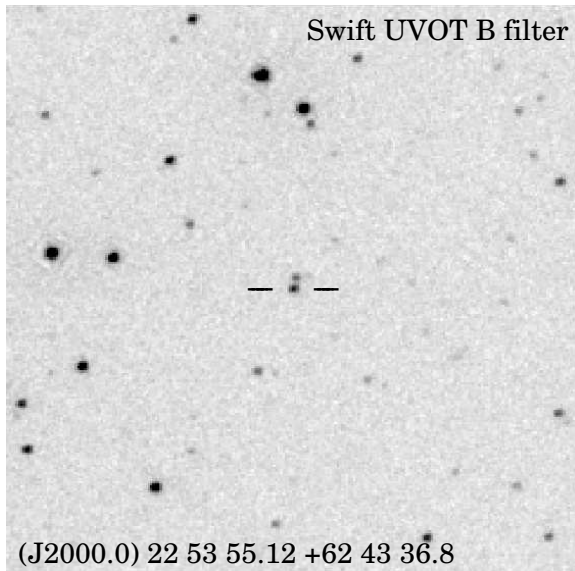
Since the 2MASS sources are slightly blended in the UVOT images (see Fig. 7), we used for the photometry a small aperture radius of 2 arcsec (no attempt was made to correct for possible residual contamination from 2MASS 22535500+6243412). The source is detected with high confidence in all the UVOT filters but the *uvm2*, in which the statistical significance of the source is only at a  $3.2\sigma$  confidence level. The average Vega UVOT magnitudes, calculated from the stacked images using the UVOTSOURCE tool, are reported in Table 5.

##### 5.1 Spectral type of the stellar companion

The optical spectrum shows the presence of H $\alpha$  (equivalent width,  $EW \sim -38 \text{ \AA}$ ), H $\beta$  ( $EW \sim -5 \text{ \AA}$ ) and H $\gamma$  ( $EW \sim -1 \text{ \AA}$ )

**Table 4.** Spectral analysis of 1RXS J2253. Errors are at a  $1\sigma$  confidence level for a single parameter of interest.

Observation	$N_{\text{H}}$ ( $10^{22} \text{ cm}^{-2}$ )	$\Gamma$	Observed flux <sup>a</sup> ( $10^{-12} \text{ erg cm}^{-2} \text{ s}^{-1}$ )	Unabsorbed flux <sup>a</sup>	$\chi^2_{\nu}$ (dof)
ROSAT 500321	$1.8^{+1.1}_{-0.7}$	$3^{+3}_{-2}$	$0.5 \pm 0.2$	$4^{+90}_{-3}$	0.60 (12)
Swift 7000	$1.7 \pm 0.2$	$1.2^{+0.2}_{-0.1}$	$4.5^{+0.3}_{-0.2}$	$6.2 \pm 0.3$	1.04 (48)
Swift 7001	$2.0 \pm 0.2$	$1.5 \pm 0.1$	$3.0 \pm 0.1$	$4.7 \pm 0.3$	1.12 (67)
Chandra 9920	$1.6^{+0.1}_{-0.2}$	$1.2 \pm 0.1$	$2.7^{+0.1}_{-0.2}$	$3.6 \pm 0.1$	0.91 (88)
Chandra 10811	$1.8 \pm 0.2$	$1.3 \pm 0.1$	$3.3 \pm 0.2$	$4.7 \pm 0.2$	0.79 (68)
Chandra 10812	$2.0 \pm 0.2$	$1.4^{+0.1}_{-0.2}$	$2.4 \pm 0.1$	$3.6 \pm 0.2$	0.84 (63)
Chandra 10810	$1.9^{+0.2}_{-0.1}$	$1.4 \pm 0.1$	$3.4^{+0.1}_{-0.2}$	$5.0 \pm 0.2$	0.94 (89)
Chandra 9919	$1.8^{+0.3}_{-0.2}$	$1.2^{+0.2}_{-0.1}$	$2.7^{+0.1}_{-0.2}$	$3.7^{+0.1}_{-0.2}$	1.24 (56)

<sup>a</sup> In the 0.5–10 keV energy range.**Figure 7.** *Swift*/UVOT *B*-band image ( $4' \times 4'$ ) centred on 2MASS 22535512+6243368 (marked with solid lines).**Table 5.** UVOT magnitudes, not corrected for the extinction. We also give the catalogued 2MASS infrared magnitudes

Filter	Magnitude	Exposure (ks)
<i>V</i>	$15.78 \pm 0.09$	7.5
<i>B</i>	$17.38 \pm 0.11$	6.4
<i>U</i>	$17.64 \pm 0.12$	9.5
<i>uvw1</i>	$19.24 \pm 0.13$	15.1
<i>uvm2</i>	$22.34 \pm 0.38$	17.2
<i>uvw2</i>	$20.54 \pm 0.16$	19.2
<i>J</i>	$11.64 \pm 0.02$	–
<i>H</i>	$10.96 \pm 0.02$	–
<i>K</i>	$10.46 \pm 0.03$	–

in emission ( $\text{H}\delta$  seems to be filled in while  $\text{He I}$  is in absorption) together with  $\text{He I}$  emission lines at 6678 Å, 5875 Å and 5016 Å (the  $\text{He I}$  at 4713 Å is likely filled in while  $\text{He I}$  at 4471 Å is in absorption) and a number of metallic lines typical of an early B-type star of low luminosity (Fig. 8). More precisely, the absence of (or very weak)  $\text{He II}$  lines indicates a spectral type later than

B1.  $\text{He I}$  lines dominate the spectrum (together with the hydrogen lines), indicating a B0 to B2 star. However, the presence of some amount of  $\text{Si III}$  4552–68 Å (the identification of this lines is unclear since we see only one of the triplet transition) and the carbon blends ( $\text{C III}$  4650 Å) favours the B0–B1 spectral type. On the other hand, the weakness/absence of the oxygen and silicon lines points toward a main-sequence star, although the strength of  $\text{C III}$  4650 Å might be a signature of a giant companion. We tentatively conclude that the optical counterpart to 1RXS J2253 is likely a B0V–B1V star (more likely a B1V), although a more luminous companion cannot be ruled out by present data.

Assuming typical colours of a B1V star,  $(B - V)_0 = -0.23$  (Wegner 1994), and comparing with the observed colour  $(B - V)_{\text{obs}} = 1.49\text{--}1.7$  (Table 5), we derived an excess colour of  $E(B - V) = 1.72\text{--}1.93$ . Assuming an absolute magnitude of  $M_V = -3.2$  (Gray & Corbally 2009), we estimate the distance to be  $\sim 4\text{--}5$  kpc (which is consistent with the Perseus arm; e.g. Russeil 2003). Similar reasoning applies for a B1I and a B1II spectral class and imply distances in the  $\sim 14\text{--}19$  kpc and  $\sim 9\text{--}12$  kpc ranges, respectively. The Galaxy edge of about 10 kpc in the direction of 1RXS J2253 rules out the possibility that the companion star is a B1I, while is marginally in agreement with a B1II spectral type (which, however, seems to be incompatible with the apparent lack of OII absorption lines at 4415–17 Å).

## 6 DISCUSSION

We reported here on the discovery of 47-s spin pulses in the X-ray emission of 1RXS J2253 and on a multiwavelength and long-term ( $\sim 16$  years) study of the source which made it possible to put stringent constraints on its nature. The optical spectroscopy indicates a B1-type companion, very likely a main sequence star at a distance of  $\sim 4\text{--}5$  kpc, implying that 1RXS J2253 can be classified as a massive X-ray binary located in the Perseus arm of our Galaxy. This estimated range for the pulsar distance translates into an X-ray luminosity of  $(2.3\text{--}3.6) \times 10^{34} \text{ erg s}^{-1}$  assuming an average flux of  $1.2 \times 10^{-11} \text{ erg cm}^{-2} \text{ s}^{-1}$  (1–60 keV, corrected for the absorption). The X-ray emission at a level of  $\approx 10^{34} \text{ erg s}^{-1}$  in observations spaced by several years, strongly suggests that 1RXS J2253 is a member of the sub-class of Be X-ray pulsars where the persistent and low X-ray luminosity is driven by the accretion onto the neutron star of wind material from the massive companion in a wide (orbital period,  $P_{\text{orb}}$ , longer than  $\sim 30$  days) and nearly circular ( $e < 0.2$ ) orbit. These sources, the prototype and most luminous of which is X Persei (White et al. 1976; Delgado-Martí et al. 2001;



been observed by *INTEGRAL*/IBIS for a net exposure time of 7.5 Ms, and no bright flares nor outbursts have ever been reported, consistently with a faint persistent source. The almost constant (within a factor of  $\sim 2$ ) X-ray luminosity (note the large uncertainty in the extrapolation of the *ROSAT* flux to higher energies) points to a circular, or nearly circular, orbit.

High mass X-ray binaries composed of neutron stars accreting from main-sequence companions are likely to constitute a not negligible fraction of the unidentified Galactic X-ray sources with relatively low luminosities,  $L_X$  less than  $10^{35}$  erg s $^{-1}$  (perhaps a few percents but less than 10%; see e.g. Laycock et al. 2005; Hong 2012). Our findings suggest that 1RXS J2253 is a new member of an elusive population of persistent low-luminosity Galactic HMXBs accreting from B main-sequence donors.

## ACKNOWLEDGMENTS

The project leading to these results has received funding from the European Union Seventh Framework Programme (FP7/2007–2013) under grant agreement No. 312430 (OPTICON). This research is based on data and software provided by the CXC (operated for NASA by SAO), the NASA's HEASARC and the ASI Science Data Center (for the *Swift* XRT Data Analysis Software, XRT-DAS), and on observations made with the NOT, operated by the NOTSA in the IAC's Observatorio del Roque de los Muchachos. We also made use of data products from the Two Micron All Sky Survey, which is a joint project of the University of Massachusetts and the IPAC/Caltech, funded by the NASA and the NSF. We thank Enrico Bozzo for useful discussions.

## REFERENCES

- Allen T. S. et al., 2012, *ApJ*, 750, 125
- Arnaud K. A., 1996, in Jacoby G. H., Barnes J., eds, *Astronomical Data Analysis Software and Systems V* Vol. 101 of *Astronomical Society of the Pacific Conference Series*. ASP, San Francisco, pp 17–20
- Bisnovatyi-Kogan G. S., 1991, *A&A*, 245, 528
- Breeveld A. A., Landsman W., Holland S. T., Roming P., Kuin N. P. M., Page M. J., 2011, in J. E. McEnery, J. L. Racusin, & N. Gehrels ed., *Gamma Ray Bursts 2010*. Vol. 1358 of *AIP Conference Proceedings*. AIP, Melville, pp 373–376
- Buccheri R. et al., 1983, *A&A*, 128, 245
- Burrows D. N. et al., 2005, *Space Science Reviews*, 120, 165
- Corbet R. H. D., 1986, *MNRAS*, 220, 1047
- Davidson K., Ostriker J. P., 1973, *ApJ*, 179, 585
- Davies R. E., Fabian A. C., Pringle J. E., 1979, *MNRAS*, 186, 779
- Davies R. E., Pringle J. E., 1981, *MNRAS*, 196, 209
- Delgado-Martí H., Levine A. M., Pfahl E., Rappaport S. A., 2001, *ApJ*, 546, 455
- Doroshenko V., Santangelo A., Kreykenbohm I., Doroshenko R., 2012, *A&A*, 540, L1
- Garmire G. P., Bautz M. W., Ford P. G., Nousek J. A., Ricker Jr. G. R., 2003, in *X-Ray and Gamma-Ray Telescopes and Instruments for Astronomy*. Edited by Truemper, J. E. and Tananbaum, H. D. Vol. 4851 of *Proceedings of the SPIE*. SPIE, Bellingham, pp 28–44
- Ghosh P., Lamb F. K., 1979a, *ApJ*, 232, 259
- Ghosh P., Lamb F. K., 1979b, *ApJ*, 234, 296
- Goad M. R. et al., 2006, *GCN Circ.*, 4985
- Gray R. O., Corbally J. C., 2009, *Stellar Spectral Classification*. Princeton University Press
- Halpern J. P., 2012, *Astron. Tel.*, 4240
- Hanuschik R. W., 1996, *A&A*, 308, 170
- Hanuschik R. W., Hummel W., Sutorius E., Dietle O., Thimm G., 1996, *A&AS*, 116, 309
- Hong J., 2012, *MNRAS*, 427, 1633
- Hummel W., Hanuschik R. W., 1997, *A&A*, 320, 852
- Illarionov A. F., Kompaneets D. A., 1990, *MNRAS*, 247, 219
- Israel G. L. et al., 2002, *A&A*, 386, L13
- Israel G. L., Panzera M. R., Campana S., Lazzati D., Covino S., Tagliaferri G., Stella L., 1999, *A&A*, 349, L1
- Israel G. L., Rodríguez G., 2012, *Astron. Tel.*, 4241
- Israel G. L., Stella L., 1996, *ApJ*, 468, 369
- Krivonos R., Tsygankov S., Lutovinov A., Revnivtsev M., Churazov E., Sunyaev R., 2012, *A&A*, 545, A27
- Kudritzki R.-P., Puls J., 2000, *ARA&A*, 38, 613
- La Palombara N., Mereghetti S., 2007, *A&A*, 474, 137
- Landi R., Bassani L., Masetti N., Bazzano A., Ubertini P., Bird A. J., Goossens M., 2012, *Astron. Tel.*, 4166
- Laycock S., Grindlay J., van den Berg M., Zhao P., Hong J., Koenig X., Schlegel E. M., Persson S. E., 2005, *ApJ*, 634, L53
- Lebrun F. et al., 2003, *A&A*, 411, L141
- Lovelace R. V. E., Romanova M. M., Bisnovatyi-Kogan G. S., 1995, *MNRAS*, 275, 244
- Marlborough J. M., 1969, *ApJ*, 156, 135
- Masetti N., Jimenez-Bailon E., Chavushyan V., Parisi P., Bazzano A., Landi R., Bird A. J., 2012, *Astron. Tel.*, 4248
- Moretti A. et al., 2005, in Siegmund O. H. W., ed., *UV, X-Ray, and Gamma-Ray Space Instrumentation for Astronomy XIV* Vol. 5898 of *SPIE Conference Series*. SPIE, Bellingham, pp 348–356
- Okazaki A. T., 1997, *A&A*, 318, 548
- Okazaki A. T., Negueruela I., 2001, *A&A*, 377, 161
- Parmar A. N., White N. E., Stella L., Izzo C., Ferri P., 1989, *ApJ*, 338, 359
- Perna R., Bozzo E., Stella L., 2006, *ApJ*, 639, 363
- Pfahl E., Rappaport S., Podsiadlowski P., Spruit H., 2002, *ApJ*, 574, 364
- Pfeffermann E. et al., 1987, in *Soft X-ray optics and technology*. Edited by E.-E. Koch & G. Schmahl Vol. 733 of *SPIE Conference Series*. SPIE, Bellingham, pp 519–532
- Poole T. S. et al., 2008, *MNRAS*, 383, 627
- Press W. H., Teukolsky S. A., Vetterling W. T., Flannery B. P., 1992, *Numerical recipes in C. The art of scientific computing*. Cambridge: University Press, 2nd ed.
- Ramsay G., Hakala P., Cropper M., 2002, *MNRAS*, 332, L7
- Rea N., Esposito P., 2011, in Torres D. F., Rea N., eds, *Astrophysics and Space Science Proceedings, High-Energy Emission from Pulsars and their Systems*. Springer, Heidelberg, pp 247–273
- Roming P. W. A. et al., 2005, *Space Science Reviews*, 120, 95
- Russeil D., 2003, *A&A*, 397, 133
- Sguera V. et al., 2005, *A&A*, 444, 221
- Shakura N., Postnov K., Kochetkova A., Hjalmarsdotter L., 2012, *MNRAS*, 420, 216
- Skrutskie M. F. et al., 2006, *AJ*, 131, 1163
- Struve O., 1931, *ApJ*, 73, 94
- Suchkov A. A., Hanisch R. J., 2004, *ApJ*, 612, 437
- Taam R. E., Brown D. A., Fryxell B. A., 1988, *ApJ*, 331, L117
- Tody D., 1993, in Hanisch R. J., Brissenden R. J. V., Barnes J., eds, *Astronomical Data Analysis Software and Systems II*



- Vol. 52 of Astronomical Society of the Pacific Conference Series. ASP, San Francisco, pp 173–183
- Ubertini P. et al., 2003, A&A, 411, L131
- Voges W. et al., 2000, IAU Circ., 7432, 3
- Waters L. B. F. M., de Martino D., Habets G. M. H. J., Taylor A. R., 1989, A&A, 223, 207
- Waters L. B. F. M., van den Heuvel E. P. J., Taylor A. R., Habets G. M. H. J., Persi P., 1988, A&A, 198, 200
- Wegner W., 1994, MNRAS, 270, 229
- Weisskopf M. C., Brinkman B., Canizares C., Garmire G., Murray S., Van Speybroeck L. P., 2002, PASP, 114, 1
- White N. E., Giommi P., Angelini L., 1994, IAU Circ., 6100, 1
- White N. E., Mason K. O., Sanford P. W., Murdin P., 1976, MNRAS, 176, 201
- White N. E., Swank J. H., Holt S. S., 1983, ApJ, 270, 711

This paper has been typeset from a  $\text{\TeX}$ / $\text{\LaTeX}$  file prepared by the author.